Patients had to have fully recovered from toxicity associated with previous therapy. Patients were ineligible for the study if they had symptomatic central nervous system metastases, neurological symptoms, fever, or unstable significant clinical conditions. Patients who were receiving corticosteroids, anticoagulants, immunotherapy, biological response modifiers, or other investigational agents; or who had received prior radiation therapy to 20% greater of bone marrow; or who had received a bone marrow stem cell transplant, were excluded from the study.

The protocol was approved by the institutional review boards of the National Cancer Center Hospital and the Nagoya Medical Center, and all patients gave written informed consent prior to study entry.

Dosage and dose escalation

Edotecarin (J-107088) was provided as an injectable preparation in plastic infusion bags by Banyu Pharmaceutical Co., Ltd. (Tokyo, Japan). Each bag contained 37.5 mg edotecarin in a 250 ml 5% glucose solution (final edotecarin concentration of 0.15 mg/ml). Edotecarin was administered by intravenous (IV) infusion over 2 h every 21 days. Patients were hospitalized for the initial course of edotecarin and remained hospitalized for close observation for 21–28 days thereafter. Subsequent courses could be administered on an outpatient basis with a weekly evaluation by the investigator.

The initial dose of edotecarin was 8 mg/m^2, and subsequent doses were escalated in approximately 33% increments (to 11 and 15 mg/m^2). Patients were enrolled in cohorts of 3 patients per dose and observed for 21 days; the observation period was extended to 28 days if a longer recovery period was needed. If only one of the three patients experienced a dose-limiting toxicity (DLT), then three additional patients were treated at the same dose. If none of the first three patients in a cohort, or if only one of six patients demonstrated DLT, then the next three patients were treated at the next higher dose. If at least two patients in the cohort experienced DLT, that dose level was regarded as the MTD. The dose for the next cohort would then be reduced by approximately 15%. The recommended dose for future Phase II studies was to be evaluated in a total of nine patients and was to be the highest dose at which fewer than a third of treated patients experienced a DLT. Individual patients who did not experience DLT and had no evidence of disease progression could receive up to four courses of edotecarin at the dose originally assigned. No intrapatient dose escalation was permitted. Patients who had a DLT that had recovered to grade 2 or less could continue treatment with edotecarin at a dose below the dose at which DLT was demonstrated. If DLT occurred at the reduced dose, no further treatment was to be administered. Patients with progressive disease were to discontinue treatment.

Definition of dose limiting toxicity (DLT)

For the purpose of this study, DLT was defined as the occurrence of pre-specified severe adverse events [severity defined according to the National Cancer Institute Common Toxicity Criteria (NCI CTC) version 2.0], occurring during cycle 1 and attributed to edotecarin. Criteria that are relevant to DLT's observed in this study were: grade 3 or 4 non-hematologic toxicity (except nausea, vomiting, fever and fatigue effectively managed with symptomatic treatment, and alopecia); grade 4 granulocytopenia accompanied by fever of ≥39.1°C, or accompanied by an infection requiring antibiotic or antifungal treatment based on fever of ≥38.0°C, or that persisted ≥5 days; grade 4 leukopenia that persisted ≥5 days; or failure of granulocyte and platelet counts to return to ≥1,500/mm^3 and ≥100,000/mm^3, respectively, within 28 days after edotecarin administration.

Supportive care

Each patient received granisetron 3 mg and dexamethasone 20 mg IV pretreatment on day 1 and dexamethasone 8 mg IV on days 2–4 post treatment for prevention of nausea, vomiting, and general malaise. Granisetron 3 mg IV was also administered on days 2–4 if needed. Routine use of colony-stimulating factors was not permitted during cycle 1. However, patients who had granulocytopenia that had met the criteria for DLT were permitted to receive filgrastim in cycle 1 and subsequent cycles.

Patient evaluation

Patients were evaluated at baseline and periodically throughout the study. During the first cycle, vital signs were measured every 1–3 days, hematology determinations were performed every 2–3 days, and serum biochemistries on days 3, 8, and 15. Physical examinations, including evaluation of performance status and measurement of palpable tumors, were done on days 8 and 15. During the second and the subsequent cycles, vital signs, laboratory tests and toxicity evaluations were performed on days 1, 8, and 15 of each cycle. For cycle 1, blood coagulation studies were done before each dose and on days 8 and 15. Measurements for subsequent cycles were on day 1, and finally, within 2 weeks after terminating the study. Performance status was assessed by the physician according to the ECOG criteria [14]. Tumor responses were based on WHO criteria. Radiographic evaluations of tumor size were performed every two cycles and were to be repeated after 4 weeks in case of response. Safety events were recorded on the basis of changes in signs and symptoms, physical findings, vital signs, and laboratory abnormalities. Weekly severity

assessments of subjective and objective findings were performed according to the NCI CTC version 2.

Plasma edotecarin measurements and assay

Pharmacokinetic analysis

Pharmacokinetic studies were performed during the first cycle of treatment. On day 1, blood samples (6 ml each) were drawn into heparinized tubes from an indwelling IV cannula in the arm contralateral to the arm bearing the infusion line. Samples were collected before infusion, at 15 and 60 min after the start of the infusion, at the end of the 2-h infusion, and at 5, 15, 30, and 60 min and 2, 4, 6, 8, 10 and 24 h after the end of the infusion. Urine samples were collected over two 24-h intervals for 48 h after the start of the infusion.

The concentrations of edotecarin in plasma and in urine were analyzed by Mitsubishi Chemical BCL (Tokyo) using validated, high-performance liquid chromatography. J-109404, a chemical analog of edotecarin, was the internal standard. BondElut CH cartridges were pre-conditioned with successive 1-ml washes of dichloromethane, methanol, and water. Plasma samples (1 ml) were mixed with 0.1 ml of 10% acetonitrile, 0.1 ml of the internal standard (1 μg/ml) in 10% acetonitrile, and 1 ml of 50 mM, pH 7.0 phosphate buffer and applied to pre-washed BondElut cartridges. The cartridges were then washed with 1 ml of water, spun at 1,000 rpm for 1 min at 4°C, washed again with 1-ml of 20% methanol, and spun again. To each column was then added 0.5 ml of 60% methanol followed by centrifugation to elute the retained compounds of interest. Eluates were dried under a nitrogen stream, reconstituted in 0.1 mL of mobile phase, and transferred to Ultrafree MC (0.2 μm) centrifugal filter units. The filter units were spun at 15,000 rpm for 5 min at 4°C and 60 μl of the filtrate was chromatographed. Chromatography was carried out on a Superiorex ODS S-5 μm, 4.6 mm ID×250 mm column with a Capcell C18 UG120, 4 mm ID×10 mm guard cartridge (source of columns was Shiseido, Tokyo) eluted with water/acetonitrile/methanol/trifluoroacetate (TFA) (67/18/15/0.1) flowing at 1.0 ml/min. The ultraviolet absorbance of the effluent was monitored at 334 nm. Linearity was demonstrated over the range of 1–500 ng/ml. Assays of quality control samples (each assay run included 2 replicate QC samples each at 2.5, 40.0, and 400.0 ng/ml) were within ±20% of nominal concentrations, with one exception: a single 2.5 ng/ml replicate assayed at 1.6 ng/ml in 1 assay run. The lower limit of quantitation (LLOQ) was 1.0 ng/ml. The interday and intraday coefficients of variation for plasma are 2.0~5.9% and 2.0~4.0%, respectively.

Extraction and chromatography of urine samples was carried out with slight modifications of the plasma method. The urine volume assayed was 0.1 ml, which was mixed with 0.1 ml of 10% acetronitrile, 0.1 ml of 2 μg/ml internal standard in 10% acetonitrile, and 0.2 ml of mM phosphate buffer, pH 7.0. Extraction was carried out using pre-washed BondElut CN columns. The mobile phase consisted of acetonitrile/water/TFA (75/25/0.1) flowing at 0.8 ml/min. The absorbance of the effluent was monitored at 430 nm. LLOQ was 50 ng/ml. Performance of the urine assay was comparable to that of the plasma assay. The interday and intraday coefficients of variation for urine are 1.1~8.5 and 3.3~6.6%, respectively.

Adequate freeze/thaw, frozen storage, and autosampler stability were demonstrated for both plasma and urine samples. Stability for plasma and urine was demonstrated after three cycles of freezing and thawing; at −70°C for 3.5 months; and for 24 h while in the autosampler during the assays.

Statistical analysis

Noncompartmental pharmacokinetic parameters were computed using WinNonlin, version 3.1 software (Pharsight Corporation, Mountain View, CA, USA) [15]. An apparent terminal half-life ($t_{1/2}$) was calculated from plasma concentrations observed at 8, 10, and 24 h after the end of the infusion. Dose proportionality was analyzed by means of a power model: $AUC_{0-\infty} = A \times dose^B$ and $C_{max} = C \times dose^D$, where A and C are proportionality constants, dose units are milligram/patient, and the 95% confidence limits around B and D include 1 if AUC and C_{max} are directly proportional to dose. Nonlinear regression of $AUC_{0-\infty}$ and C_{max} versus dose and 95% confidence limits on computed parameters B and D were computed using GraphPad Prism, version 4 (GraphPad Software, San Diego, CA, USA). Descriptive statistics (Table 6) were also computed using GraphPad Prism.

Results

Patient characteristics

Twenty-four Japanese patients were enrolled into the study (Table 1) and received at least one dose of edotecarin. The median age of the patients was 56 years (range 33–72), 22 (92%) had an ECOG performance status of 1 at baseline, and 16 (67%) patients were male. The most common tumor types were lung and colorectal cancer. All patients except one had previously received chemotherapy with a median number of chemotherapy regimens of 2 (range 0–4). Patients treated at various dose levels had similar baseline characteristics.

All 24 patients were assessed for both safety and efficacy.

A total of 61 cycles of treatment were administered in these patients. The majority of cycles were administered every 3 weeks, with 10 cycles administered at day 28. Three cycles were administered beyond this to accommodate patients' personal reasons and schedules. The

Table 1 Patient characteristics

Number enrolled	24
Age (years)	
Median	56
Range	33–72
Male:female (no. of patients)	16:8
ECOG performance status (no. of patients)	
0	2
1	22
Tumor type (no. of patients)	
Lung	7
Colorectal	4
Uterine sarcoma	3
Gastric	2
Bile duct	2
Primary unknown	2
Other	4
Prior treatment	
Chemotherapy	
No. of prior regimens (no. of patients)	
0	1
1	11
2	8
3	3
4	1
Median (no. of regimens)	2
Surgery (no. of patients)	11
Radiation therapy (no. of patients)	5
Chemotherapy + radiation therapy (no. of patients)	5

median number of cycles at the 13 mg/m^2 dose was 2 (range 1–6). The most common reasons for treatment discontinuation were progressive disease or best response achieved (i.e., further treatment effect not expected) (nine patients each) (Table 2).

Dose escalation and identification of DLT, MTD, and the recommended Phase II dose

At the initial dose of 8 mg/m^2, no patient experienced DLT. At the next dose of 11 mg/m^2, 1 of 6 patients experienced DLTs (grade 3: infection, febrile neutropenia, and hypoxia). Six patients were enrolled at 15 mg/m^2. Three patients experienced DLTs (grade 3: infection, febrile neutropenia, and constipation in 1 patient; grade 3: ileus and constipation in the second; and grade 4 granulocytopenia persisting for 5 days or more in the third). Both patients who had grade 3 constipation had previous intestinal surgery for rectal and colon cancer, respectively. One patient with superior vena caval syndrome at baseline required radiotherapy at day 7 for progression of this syndrome. The dose of 15 mg/m^2 was defined as the MTD.

Consequently, 9 patients were treated at 13 mg/m^2. Two of the nine patients treated at this dose experienced DLTs (grade 4 granulocytopenia persisting for 5 days or more in both patients). Therefore, based on protocol-predefined criteria, 13 mg/m^2 is the dose recommended for future single-agent Phase II studies with an administration every 21 days (with an additional week permitted for recovery from toxicities, if needed).

Non-hematologic toxicity

The non-hematologic adverse events reported most commonly (occurrence in ≥50% of all patients treated) during the first cycle were anorexia, nausea, malaise, and constipation (Table 3). No grade 4 non-hematologic toxicities were reported in any treatment group. During subsequent cycles, adverse events were similar in terms of frequency and severity to those reported during the first cycle of treatment and no cumulative toxicity was observed.

Gastrointestinal toxicity, usually mild, was the most common non-hematologic toxicity associated with edotecarin administered with an antiemetic regimen. The median time to onset of constipation during the first cycle was 3 days (range: 2–4 days). None of the patients who received antiemetic prophylaxis and who were treated at the Phase II recommended dose of 13 mg/m^2 had grade 2 or higher nausea, vomiting, or anorexia. Diarrhea (grade 1–2) was observed in only a few patients (8 mg/m^2, 1 patient; 11 mg/m^2, 2; 13 mg/m^2, 2; and 15 mg/m^2, 1). Alopecia was not reported. Injection site phlebitis (grade 2) was reported in 11 (48%) of the patients. The frequency of this event was not dose-dependent, suggesting that it was related to the infusion

Table 2 Number of treatment cycles, number of patients with dosing interval extensions and reasons for treatment discontinuation

	Edotecarin dose (mg/m^2)			
	8	11	13	15
Number of patients	3	6	9	6
Median number of treatment cycles (range)	3 (1–4)	2 (1–4)	2 (1–6)	1 (1–5)
Dose delay				
Number of patients (number of days in dosing interval)	0	1 (45)	2 (31–34)	0
Reasons for treatment discontinuation				
Progressive disease	1	3	4	1
Further treatment effect not expected	2	2	3	2
DLT	0	1	1	2
Adverse events other than DLT	0	0	1	0
Prohibited concomitant therapy	0	0	0	1

Table 3 Most common non-hematologic toxicities occurred in ≥50% of all patients treated during cycle 1

Adverse event	Grade	Dose (mg/m^2)				All doses ($N=24$)
		8 ($N=3$)	11 ($N=6$)	13 ($N=9$)	15 ($N=6$)	
Anorexia	1/2	3 (100%)	6 (100%)	7 (78%)	4 (67%)	20 (83%)
	3/4	0	0	0	0	0
Nausea	1/2	2 (67%)	2 (33%)	5 (56%)	6 (100%)	15 (63%)
	3/4	0	1 (17%)	0	0	1 (4%)
Malaise	1/2	3 (100%)	4 (66%)	5 (56%)	4 (67%)	16 (67%)
	3/4	0	0	0	0	0
Constipation	1/2	1 (33%)	1 (17%)	6 (67%)	3 (50%)	11 (46%)
	3/4	0	0	0	2 (33%)	2 (8%)

procedure rather than the drug. There were no deaths within 28 days of edotecarin administration, and none of the deaths that occurred after the study were considered treatment-related.

One adverse event deserves a more detailed description. A 44 year-old-male with esophageal cancer with liver and lung metastases developed grade 2 interstitial pneumonitis 2 weeks after administration of edotecarin 13 mg/m^2. He had undergone radiation therapy for the primary lesion approximately 4 months before edotecarin infusion. Most lesions of the interstitial pulmonary lesions were in the field of radiation therapy, and radiation pneumonitis was diagnosed. However, the rapid onset of pneumonitis after edotecarin infusion suggested a recall phenomenon induced by edotecarin and the event was judged to be possibly related to the study treatment.

Hematologic toxicity

Neutropenia/granulocytopenia, leukopenia, anemia, and lymphocytopenia were the most common (occurrence in ≥50% of all patients treated at the 3 highest dose levels) hematologic toxicities reported during the first cycle (Table 4). Neutropenia was the principal hematologic toxicity in this study and granulocytopenia was dose-limiting at 13 and 15 mg/m^2 (Table 5). At 11–15 mg/m^2, the median time to nadir granulocyte count was 11–14 days, and the median time to recovery from nadir was 5 to 7 days. In all patients, granulocyte counts recovered to grade 1 within 21 days after edotecarin infusion at 8 and 15 mg/m^2, but had not recovered by day 22 in 1 patient at 11 mg/m^2 and in 4 patients at 13 mg/m^2. However, by day 26 after edotecarin infusion, granulocyte counts were within normal limits in all patients. Given this frequent and severe neutropenia, G-CSF support was provided during cycle 1 in 2 patients at 13 mg/m^2 and 1 at 15 mg/m^2,after DLT confirmation. Grade 4 granulocytopenia persisting for more than 5 days led to dose reduction in the second cycle in 2 patients, one each at 13 and 15 mg/m^2.

Grade 4 neutropenia (not necessarily lasting > 5 days), was reported in 15 (65%) patients during the first cycle of therapy, and was observed at all dose levels but did not increase in incidence with additional cycles.

Anemia, reported in 15 (65%) patients, did not exceed grade 1 or 2 in severity. Thrombocytopenia was not reported in this study. The numbers of patients with abnormal laboratory values did not tend to increase with increasing courses of treatment, suggesting that the toxicity of edotecarin was not cumulative.

No significant changes were demonstrated by the blood coagulation studies, which assessed prothrombin time (PT) and activated partial thromboplastin time (aPTT).

Pharmacokinetics

Plasma pharmacokinetic parameters are listed in Table 6. Edotecarin plasma concentrations rose rapidly

Table 4 Most common hematologic toxicities occurred in ≥50% of patients at each of the three highest dose levels during cycle 1

Adverse event	Grade	Dose, mg/m^2				All doses ($N=23$)
		8 ($N=3$)	11 ($N=6$)	13 ($N=9$)	15 ($N=5$)	
Neutropenia	1/2	1 (33%)	0	0	0	1 (4%)
	3/4	1 (33%)	6 (100%)	9 (100%)	6 (100%)	22 (92%)
Granulocytopenia	1/2	1 (33%)	0	0	1 (17%)	2 (8%)
	3/4	1 (33%)	6 (100%)	9 (100%)	5 (83%)	21 (88%)
Leukopenia	1/2	1 (33%)	4 (67%)	5 (56%)	2 (33%)	12 (50%)
	3/4	0	2 (33%)	4 (44%)	4 (67%)	10 (42%)
Anemia	1/2	3 (100%)	4 (67%)	5 (56%)	4 (67%)	16 (67%)
	3/4	0	0	0	0	0
Lymphocytopenia	1/2	1 (33%)	4 (67%)	4 (44%)	2 (33%)	11 (46%)
	3/4	0	0	1 (11%)	2 (33%)	3 (13%)

Table 5 Granulocytopenia during cycle 1

Dose (mg/m²)	No. of patients	Grade				Nadir (no./mm³)[a]	Days to nadir[a]	Days to recovery (grade 0) from nadir			
								Without G-CSF		With G-CSF	
		1	2	3	4			No. of patients	No. of days[a]	No. of patients	No. of days[a]
8	3	0	0	1 (33%)	0	2,193 (550–993)	18 (14–21)	1	7	0	–
11	6	0	0	2 (33%)	4 (67%)	440 (150–923)	14 (11–16)	6	7 (3–12)	0	–
13	9	0	0	4 (44%)	5 (56%)	480 (46–912)	14 (9–21)	7	7 (2–13)	2	5 (4–5)
15	6	0	1 (17%)	2 (33%)	3 (50%)	529 (88–1,017)	11 (11–14)	4	5 (2–7)	1	5

G-CSF granulocyte colony-stimulating factor
[a]Expressed as median (range)

Table 6 Pharmacokinetic parameters in cycle 1 (mean ± SD)

Dose (mg/m²)	No. of patients[c]	C_{max}, (ng/ml)	$AUC_{0\text{-}26h}$, (ng h/ml)	$AUC_{0\text{-}\infty}$ (ng h/ml)	Percentage of area extrapolated	CL		$t_{1/2}$ (h)	V_{SS} (l/m²)	48-h urinary recovery (%)
						ml/min/m²	ml/min			
8	2	57 ± 17[a]	132, 192	330, 198	42, 23	404, 673	735, 1043	45.5, 29.0	972, 715	1.4 ± 2.3[a]
11	5	86 ± 10[b]	211 ± 38	294 ± 54	25 ± 8	624 ± 114	962 ± 287	26.1 ± 3.3	670 ± 277	3.6 ± 2.7
13	9	103 ± 17	262 ± 43	330 ± 44	19 ± 6	657 ± 88	1154 ± 138	22.9 ± 2.1	569 ± 256	2.9 ± 3.8
15	5	113 ± 17[b]	269 ± 56	352 ± 62	20 ± 5	711 ± 123	1057 ± 190	20.2 ± 1.6	561 ± 258	1.8 ± 3.4[b]

C_{max}, maximum plasma concentration; *AUC* area under the plasma concentration-time curve; *CL* clearance; $t_{1/2}$, apparent terminal half-life; V_{ss}, steady-state volume of distribution
[a]$N = 3$
[b]$N = 6$
[c]As drug concentrations were below the detectable range at one or more time points beyond the 8 h after the administration, some parameters are not available for all patients

at the start of the infusion and dropped sharply at discontinuation of the infusion (Fig. 2), reaching levels of 1–2 ng/ml at the last sampling point.

In order to compare PK data from this study, to PK data from the similar US study, a noncompartmental model for calculating PK parameters was used.

Peak plasma concentrations of edotecarin and $AUC_{0\text{-}26h}$ increased with increasing dose (Fig. 3). Power model fitting to $AUC_{0\text{-}\infty}$ and C_{max} vs dose data suggested that C_{max} was proportional to dose while $AUC_{0\text{-}\infty}$ was somewhat less than dose-proportional (results not presented).

Clearance (CL) values were comparable at 11, 13 and 15 mg/m² as were volumes of distribution.

An apparent terminal half-life ($t_{1/2}$) was calculated from plasma concentrations observed at 8, 10, and 24 h after the end of the infusion. In three patients, the plasma concentration at 1 or more of these time points was below the lower limit of quantification of 1 ng/ml; consequently, values of $t_{1/2}$, $AUC_{0\text{-}\infty}$, and CL were not calculated in these patients. The mean apparent $t_{1/2}$ was approximately 20 h. Since the PK sampling duration was only 26 h post start of infusion (i.e., for only about 1 half-life), the computed $AUC_{0\text{-}\infty}$, CL, and $t_{1/2}$ values should be considered preliminary until data are available from trials measuring plasma levels through at least 3–4 times the apparent terminal $t_{1/2}$.

Mean 48-h urinary excretion accounted for 1.4–3.6% of the administered dose of edotecarin in the 4 cohorts.

Coefficient of interpatient variation in edotecarin C_{max} and AUC values was 15–20%.

Antitumor activity

All 24 patients were assessable for efficacy, and 21 patients had evaluable lesions. No objective and confirmed responses were observed. However, stable disease (SD) was reported in 12 patients (57%), with a maximum duration of 5 cycles. Eight (38%) patients had tumor volume reductions ranging from 10.5 to 65.4% based on the sum of the products of the dimensions of measurable lesions. Two patients had a decrease in tumor volume of at least 50%. One patient, enrolled at 13 mg/m², had esophageal cancer with liver metastases. After cycle 1, at day 18, tumor volume was reduced by 65%. Unfortunately, treatment was discontinued because of pneumonitis and the disease had progressed 28 days later. The second patient, who received 11 mg/m², had gastric cancer with measurable metastatic lesions in the lung

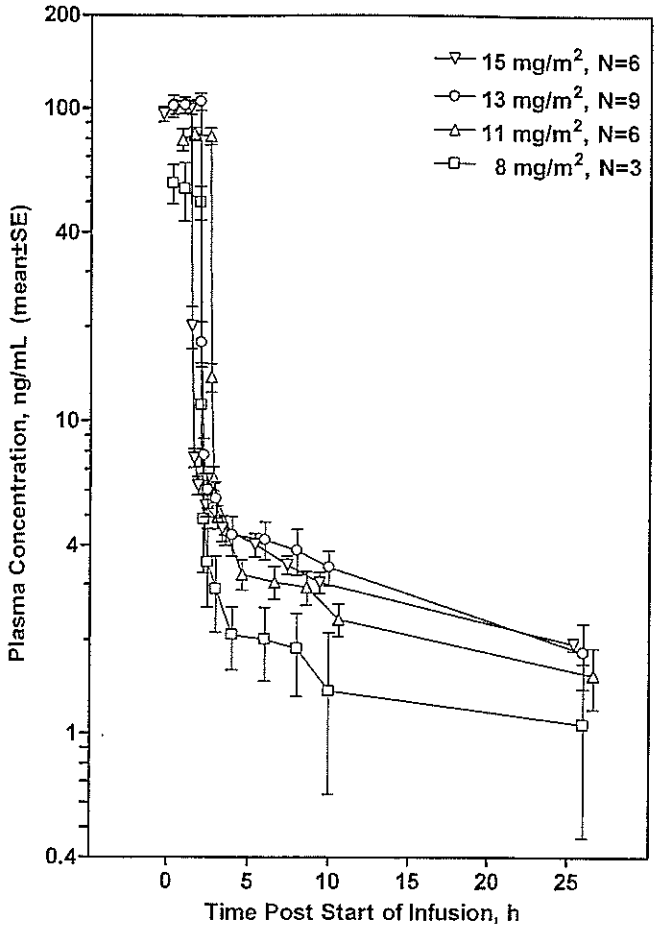

Fig. 2 Edotecarin cycle-1 plasma concentration-time profiles (mean ± SE) in patients with advanced solid tumors. Data at 11 and 13 mg/m^2 have been offset by +0.6 and −0.6 h, respectively, in the *x*-direction to prevent overlapping *data points* and *error bars*

and mediastinal lymph nodes. These lesions decreased gradually in size, with the reduction from baseline reaching 53% by cycle 3. For administrative reasons, cycle 4 was delayed (45 days). The response was no longer present and the treatment was discontinued. Three of four patients with colorectal cancer, all with lung lesions and having received prior 5-fluorouracil treatment, showed evidence of tumor stabilization.

Discussion

The first objective of this Phase I clinical study was to determine the MTD of single-agent edotecarin administered by IV infusion over 2 h once every 21 days with pre- and post-treatment supportive medication (steroids and 5-HT$_3$ antagonists). The MTD was 15 mg/m^2 with this schedule of administration. At this dose, hematologic (neutropenia, febrile neutropenia) and non-hematologic (constipation, ileus, infection without neutropenia) grade 3 and 4 toxicities were observed in 3 of the 6 patients of the MTD cohort.

In order to make a recommendation regarding the dose of edotecarin to be studied in future single-agent Phase II studies, 9 patients were treated at 13 mg/m^2 with supportive medication. Grade 4 granulocytopenia, lasting for 5 days or more, was observed in only 2 patients. Therefore this dose is recommended, with supportive medication, for future Phase II studies. A similar Phase I edotecarin trial conducted in the USA recommended the same dose [12].

At the recommended dose of 13 mg/m^2, edotecarin, infused IV for 2 h with supportive medication, had manageable toxicities. Neutropenia was dose-dependent

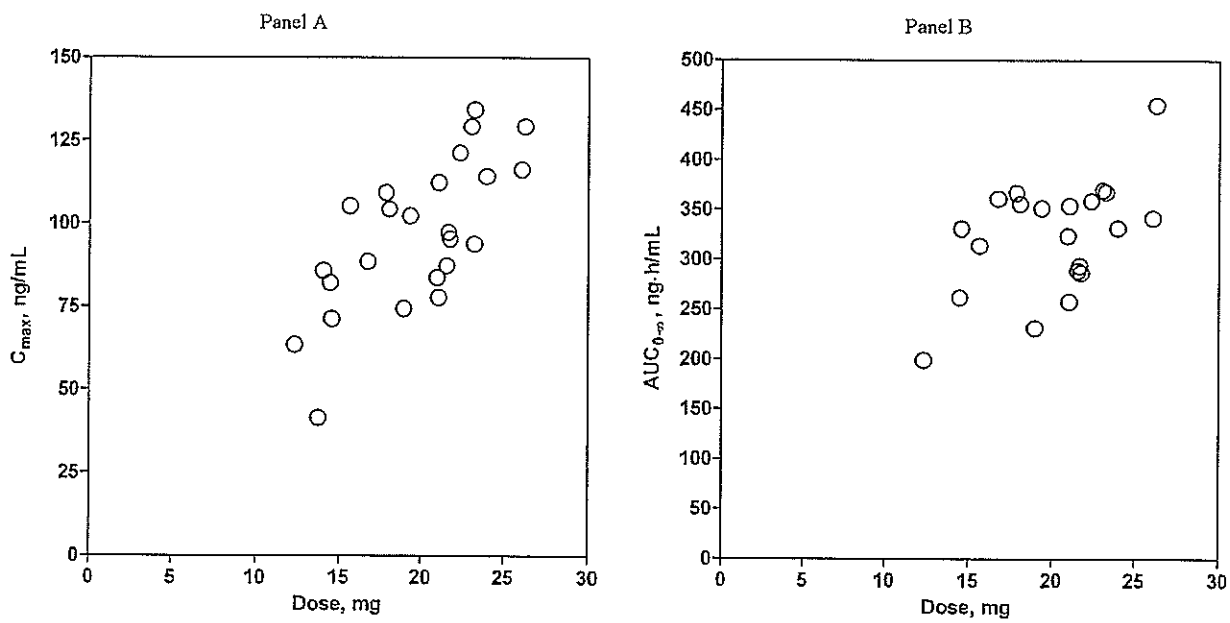

Fig. 3 Peak plasma concentrations (*left panel*) and $AUC_{0-\infty}$ values (*right panel*) as a function of dose in milligram in patients with advanced solid tumors

but was not cycle-dependent. At the recommended dose, the median time to neutrophil nadir was 14 days with a median recovery time of 7 days. This suggests that administration of edotecarin every 3 weeks is possible, but bone marrow recovery has to be verified before the administration of the next cycle. Other hematologic toxicities were observed (anemia, lymphocytopenia), but thrombocytopenia was not reported.

Gastrointestinal toxicity, the most common non-hematologic toxicity observed, was usually mild. At the recommended dose and with antiemetic premedication, nausea, vomiting or anorexia never exceeded grade 1. The incidence of constipation was dose dependent and dose-limiting at 15 mg/m^2 in 2 patients that had previously undergone intestinal surgery for cancer. However, at the recommended dose, constipation was never more severe than grade 2. In two previous Phase I trials of edotecarin [12, 13], constipation was not dose-limiting. The reason for these discrepant observations is unclear, but constipation is not infrequent in colorectal cancer patients receiving chemotherapy. For instance, the incidence of constipation in colorectal patients treated with irinotecan single agent in second line therapy is estimated between 8 and 10% [16]. Because of the relatively high frequency and the dose dependency observed in this study, frequency of bowel movements should be monitored in patients enrolled in future studies with edotecarin. Alopecia and severe diarrhea frequently observed in association with other chemotherapy drugs (e.g., camptothecins) were not seen in this trial.

At the recommended dose, 1 patient, who had received thoracic radiotherapy for lung metastasis of an esophageal carcinoma, had a grade 2 interstitial pneumonitis shortly after edotecarin infusion, suggesting a recall phenomenon. Interstitial pneumonitis has also been observed after irinotecan [17, 18]. Pulmonary toxicity should be closely monitored in patients previously treated with thoracic radiation therapy in future Phase II trials of edotecarin.

Conclusions, based on the pharmacokinetic data, are tentative because of the narrow dose range and small number of patients studied in this trial, as well as the relatively short duration of PK sampling. While plasma concentrations appeared to reach a plateau during the 2-h infusion, attainment of a steady state concentration (C_{ss}) would not be expected for a drug with the multi-compartmental disposition behavior exhibited in Fig. 2. In theory, an infusion duration of 3–4 times the apparent terminal $t_{1/2}$ of 20 h would be required to achieve C_{ss}. This is supported by the fact that an attempt to compute CL by the equation $CL = k_0/C_{max}$, where k_0 is infusion rate and C_{max} is used as an estimate of C_{ss}, yielded CL values much higher than those calculated by means of $CL = dose/AUC_{0-\infty}$ (results not presented).

Within the limited dose range of 11–15 mg/m^2, C_{max} and AUC appeared to increase roughly linearly with dose, and CL was not relatively changed. These results suggest that edotecarin exhibits linear pharmacokinetics within 11–15 mg/m^2.

Urinary recovery did not appear to vary with the dose, which indicates that renal elimination contributes minimally to total body CL.

The pharmacokinetic profile of edotecarin appears to be simple with relatively little interpatient variability compared to that of irinotecan (a prodrug topo-I inhibitor with a very complex disposition) and to many other cytotoxic drugs.

Efficacy was a secondary endpoint of this trial conducted in a population of heavily pretreated cancer patients. No partial or complete confirmed responses were observed. However 8 patients had minor reductions in tumor size, including 2 patients with >50% regression of tumor size, however these reductions were not confirmed. Twelve patients qualified as having SD. Further clinical work is necessary to quantify precisely the level of edotecarin antitumor activity.

In conclusion, this study showed that the MTD of edotecarin, administered as a 2 h infusion with supportive medication of steroids and antiemetics, is 15 mg/m^2 and the dose to be studied in future Phase II trials as a single agent with an administration every 21 days is 13 mg/m^2. At 13 mg/m^2, toxicities, mainly neutropenia, are manageable and are characterized by the lack of severe diarrhea. The pharmacokinetic profile is attractive. Edotecarin is a promising new anticancer agent, especially in colorectal cancer, and deserves further clinical evaluation.

Acknowledgements We acknowledge Ms. Sayaka Miyahara, Dr. Mami Matsumoto, Ms. Yoko Kawamura, Mr. Katsuhiro Mizuno, and Mr. Naoyoshi Yatsuzuka for pharmacokinetic analyses, data management, and clinical research coordination, and Drs. Claude George and Samit Hirawat for their contribution in preparation of this manuscript.

References

1. Takimoto CH, Arbuck SG (1996) The camptothecins. In: Chabner BA, Longo DL (eds) Cancer chemotherapy and biotherapy; principles and practice. Lippincott-Raven, Philadelphia, pp 463–484
2. Pommier Y, Pourquier P, Fan Y et al (1998) Mechanism of action of eukaryotic DNA topoisomerase I and drugs targeted to the enzyme. Biochim Biophys Acta 1400:83
3. Douillard JY, Cunningham D, Roth AD et al (2000) Irinotecan combined with fluorouracil compared with fluorouracil alone as first-line treatment for metastatic colorectal cancer: A multicentre randomised trial. Lancet 355:1041–1047
4. Saltz LB, Cox JV, Blanke C et al (2000) Irinotecan plus fluorouracil and leucovorin for metastatic colorectal cancer. N Engl J Med 343:905–914
5. Noda K, Nishiwaki N, Kawahara M et al (2002) Irinotecan plus cisplatin compared with etoposide plus cisplatin for extensive small-cell lung cancer. N Engl J Med 346:85–91
6. Cunningham D, Pyrhonen S, James RD et al (1998) A Phase III multicenter randomized study of CPT-11 versus supportive care alone in patients with 5FU-resistant metastatic colorectal cancer. Lancet 352:1413–1418

7. Yoshinari T, Matsumoto M, Arakawa H et al (1995) Novel antitumor indolocarbazole compound 6-*N*-formylamino-12,13-dihydro-1,11-dihydroxy-13-(β-D- glucopyranosyl) 5H-indolo[2,3-a] pyrrolo[3,4-c]carbazole-5,7-(6H)-dione (NB-506): induction of topoisomerase I-mediated DNA cleavage and mechanism of cell line-selective cytotoxicity. Cancer Res 55:1310–1315
8. Yoshinari T, Ohkubo M, Fukasawa K et al (1999) Mode of action of a new indolocarbazole anticancer agent, J-107088, targeting topoisomerase I. Cancer Res 59:4271–4275
9. Fukasawa K, Komatani H, Hara Y et al (1998) Sequence-selective DNA cleavage by topoisomerase I poison NB-506. Int J Cancer 75:145–150
10. Arakawa H, Morita M, Kodera T et al (1999) *In vivo* antitumor activity of a novel indolocarbazole compound, J-107088, on murine and human tumors transplanted into mice. Jpn J Cancer Res 90:1163–1170
11. Cavazos CM, Keir ST, Yoshinari T et al (2001) Therapeutic activity of the topoisomerase 1 inhibitor J-107088 [6-*N*-(1-hydroxymethyla-2-hydroxyl)ethylamino-12,13-dihydro-13-(beta-D-glucopyranosyl)-5H-indolo[2,3-a]-pyrrolo[3,4-c]-carbazole-5,7(6H)-dione]] against pediatric and adult central nervous system tumor xenografts. Cancer Chemother Pharmacol 48:250–254
12. Peck RA, Hurwitz H, Cohen RB et al (2000) Phase I trial of J-107088, a novel topoisomerase I inhibitor, administered once every 21 days. Proc Am Soc Clin Oncol 19:197a (abstract #767)
13. Lewis LD, Perez RP, Petros WP et al (2000) A Phase I study of the novel topoisomerase I inhibitor J-107088 administered on a multiple dose schedule. Proc Am Soc Clin Oncol 19:177a (abstract #688)
14. Oken MM, Creech RH, Tormey DC et al (1982) Toxicity and response criteria of the Eastern Cooperative Oncology Group. Am J Clin Oncol 5:649–655
15. Gibaldi M, Perrier D (1982) Pharmacokinetics, 2nd edn. Marcel Dekker, New York
16. Camptosar US prescribing information: http://pfizer.com/do/medicines/mn_uspi.html#c Accessed 4 July 2003
17. Fukuoka M, Niitani H, Suzuki A et al (1992) A Phase II study of CPT-11, a new derivative of camptothecin, for previously untreated non-small-cell lung cancer. J Clin Oncol 10:16–20
18. Madarnas Y, Webster P, Shorter AM et al (2000) Irinotecan-associated pulmonary toxicity. Anticancer Drugs 11:709–713

Biochem. J. (2006) 397, 537–543 (Printed in Great Britain) doi:10.1042/BJ20051962

In-frame deletion in the EGF receptor alters kinase inhibition by gefitinib

Kazuko SAKAI*†, Hideyuki YOKOTE‡, Kimiko MURAKAMI-MUROFUSHI†, Tomohide TAMURA§, Nagahiro SAIJO§ and Kazuto NISHIO*‡[1]

*Shien-Lab, National Cancer Center Research Institute, Tsukiji 5-1-1, Chuo-ku, Tokyo 104-0045, Japan, †Department of Biology, Faculty of Science, Ochanomizu University, 2-1-1 Ohtsuka, Tokyo 112-8610, Japan, ‡Pharmacology Division, National Cancer Center Research Institute, Tsukiji 5-1-1, Chuo-ku, Tokyo 104-0045, Japan, and §Medical Oncology, National Cancer Center Hospital, National Cancer Center Research Institute, Tsukiji 5-1-1, Chuo-ku, Tokyo 104-0045, Japan

The existence of an in-frame deletion mutant correlates with the sensitivity of lung cancers to EGFR (epidermal growth factor receptor)-targeted tyrosine kinase inhibitors. We reported previously that the in-frame 15-bp deletional mutation (delE746–A750 type deletion) was constitutively active in cells. Kinetic parameters are important for characterizing an enzyme; however, it remains unclear whether the kinetic parameters of deletion mutant EGFR are similar to those of wild-type EGFR. We analysed autophosphorylation in response to ATP and inhibition of gefitinib for deletion mutant EGFR and wild-type EGFR. Kinetic studies, examining autophosphorylation, were carried out using EGFR fractions extracted from 293-pΔ15 and 293-pEGFR cells transfected with deletion mutant EGFR and wild-type EGFR respectively. We demonstrated the difference in activities between unstimulated wild-type (K_m for ATP $= 4.0 \pm 0.3$ μM) and mutant EGFR (K_m for ATP $= 2.5 \pm 0.2$ μM). There was no difference in K_m values between EGF-stimulated wild-type EGFR (K_m for ATP $= 1.9 \pm 0.1$ μM) and deletion mutant EGFR (K_m for ATP $= 2.2 \pm 0.2$ μM). These results suggest that mutant EGFR is active without ligand stimulation. The K_i value for gefitinib of the deletion mutant EGFR was much lower than that of wild-type EGFR. These results suggest that the deletion mutant EGFR has a higher affinity for gefitinib than wild-type EGFR.

Key words: autophosphorylation, epidermal growth factor receptor (EGFR), gefitinib, kinase inhibition, tyrosine kinase.

INTRODUCTION

EGFR [EGF (epidermal growth factor) receptor] is among the most important targets for lung cancer therapy, and many EGFR-targeted inhibitors have been developed [1]. These EGFR-targeted compounds inhibit the tyrosine kinase activity of EGFR by competing at the ATP-binding site [2]. Many EGFR-targeted tyrosine kinase inhibitors such as gefitinib and erlotinib have been assessed clinically [3,4]. Recently, an EGFR mutation was found in patients who responded to gefitinib, and mutant EGFR has been reported to be a determinant of the response to EGFR tyrosine kinase inhibitors [5,6]. To date, over 30 EGFR mutations including delE746–A750, L858R and delL747–P753insS, have been reported in lung cancer. These EGFR mutations, except for T790M, are considered to be of the 'gain-of-function' type. Differences exist among them; for example, constitutively active in delE746–A750 compared with hyperresponsive to ligand stimulation in L858R and delL747–P753insS, although these mutant EGFRs increase sensitivity to EGFR-targeted tyrosine kinase inhibitors [7–9]. In general, the observation of hyperresponsiveness to ligand stimulation, as in the case of L858R, raises the possibility of high affinity for ATP. We reported previously that deletion mutant EGFR was constitutively phosphorylated under unstimulated conditions, whereas wild-type EGFR was not phosphorylated until ligand stimulation [7]. The differences in cellular phenotype and sensitivity to gefitinib between deletion mutant EGFR and wild-type EGFR raise the possibility that the enzymatic properties of the deletion mutant EGFR may differ from those of wild-type EGFR. However, it remains unclear whether the kinetic parameters of deletion mutant EGFR are different from those of wild-type EGFR. In the present study, we focused on the autophosphorylation of deletion mutant EGFR, and investigated the inhibition constant of gefitinib. Technically, we used deletion mutant EGFR and wild-type EGFR extracted from ectopically expressed HEK-293 (human embryonic kidney) cells. The autophosphorylation assay reflects the native behaviour of EGFR in maintaining cellular functions.

MATERIALS AND METHODS

Reagents

Gefitinib (Iressa®, ZD1839) was provided by AstraZeneca.

Cell culture

The HEK-293 cell line was obtained from the A.T.C.C. (Manassas, VA, U.S.A.) and was cultured in RPMI 1640 medium (Sigma) supplemented with 10% heat-inactivated foetal bovine serum (Life Technologies).

Plasmid construction and transfection

Construction of the expression plasmid vector of wild-type EGFR and the 15-bp deletion mutant EGFR (delE746–A750 type deletion), which has the same deletion site as that observed in detail in PC-9 cells, has been described elsewhere [7,10,11]. The plasmids were transfected into HEK-293 cells and the transfectants were selected using Zeosin (Sigma). The stable transfectants (pooled cultures) of the wild-type EGFR and its deletion mutant were designated 293-pEGFR and 293-pΔ15 cells respectively.

Abbreviations used: EGF, epidermal growth factor; EGFR, EGF receptor; HEK-293, human embryonic kidney; 293-pEGFR, HEK-293 cells transfected with wild-type EGFR; 293-pΔ15, HEK-293 cells transfected with deletion mutant EGFR; TBS-T, Tris-buffered saline with Tween 20; TGF-α, transforming growth factor-α.

[1] To whom correspondence should be addressed (email knishio@gan2.res.ncc.go.jp).

Immunoblotting

The 293-pΔ15 and 293-pEGFR cells were treated with or without gefitinib for 3 h, stimulated with EGF (100 ng/ml) under serum-starvation conditions and then lysed for immunoblot analysis. Immunoblot analysis was performed as described previously [12]. Equivalent amounts of protein were separated by SDS/PAGE (2–15 % gradient) and transferred to a PVDF membrane (Millipore). The membrane was probed with a mouse monoclonal antibody against EGFR (Transduction Laboratories), a phospho-EGFR antibody (specific for Tyr^{1068}) (Cell Signaling Technology) as the first antibody, followed by a horseradish-peroxidase-conjugated secondary antibody. The bands were visualized with ECL® (enhanced chemiluminescence) (Amersham Biosciences).

Determination of ligand secretion by ELISA

The 293-pΔ15 and 293-pEGFR cells were cultured in 12-well plates under serum-starvation conditions. The cell culture supernatant was collected for each cell line and stored at −80 °C for further analysis. Amounts of EGF and TGF-α (transforming growth factor α) in the culture medium from each cell line were determined with a DuoSet ELISA development kit (R&D Systems). The assay was performed in triplicate according to the manufacturer's instructions.

Preparation of cell lysates for EGFR autophosphorylation

Cultivated cells, after reaching 70–80 % confluence, were starved in serum-free medium for 24 h, with or without EGF (100 ng/ml) stimulation. The cells were washed twice with ice-cold PBS containing 0.33 mM $MgCl_2$ and 0.9 mM $CaCl_2$ [PBS(+)], then lysed with lysis buffer [50 mM Tris/HCl, pH 7.4, 50 mM NaCl, 0.25 % Triton X-100, 5 mM EDTA, protease inhibitor (Roche Diagnostics) and phosphatase inhibitor (Sigma)]. For the preparation of gefitinib-treated cell lysates, cultivated cells were starved in serum-free medium for 24 h, and were then pre-incubated with 2 μM gefitinib for 3 h. Either with or without EGF stimulation (100 ng/ml), the cells were washed twice with ice-cold PBS(+) and lysed with lysis buffer. The cell lysate was centrifuged at 20000 *g* for 10 min, and the protein concentration of the supernatant was measured with a BCA (bicinchoninic acid) protein assay (Pierce).

Autophosphorylation assay

The amount of EGFR in 293-pΔ15 and 293-pEGFR cells was determined by quantitative immunoassay (R&D Systems) according to the manufacturer's instructions. The autophosphorylation assay was carried out with a quantitative immunoassay system. Wells in a 96-well immunomodule (Nalge Nunc International) were incubated with 0.8 μg/ml goat anti-(human EGFR) antibody in PBS (provided with the EGFR quantitative immunoassay system) and incubated at 4 °C overnight. The plates were washed three times with TBS-T (Tris-buffered saline with Tween 20; 20 mM Tris/HCl, pH 7.4, 150 mM NaCl and 0.05 % Tween 20) and were then filled with blocking buffer (PBS containing 1 % BSA and 5 % sucrose) and incubated for 2 h at room temperature (25 °C). The wells were washed three times with TBS-T and incubated with cell lysates of 293-pEGFR or 293-pΔ15 including equal amounts of EGFR (130 ng of EGFR/well) diluted with lysis buffer. After a 2 h incubation at room temperature, the 96-well plate was washed with TBS-T. Autophosphorylation of EGFR was initiated by addition of ATP (0–32 μM in 50 mM Tris/HCl, pH 7.5, 20 mM $MgCl_2$ and phosphatase inhibitor) followed by incubation for 5 min. In some experiments, various concentrations of gefitinib were added to the wells before the addition of ATP. Following the autophosphorylation reaction, the wells were washed with TBS-T. Next,

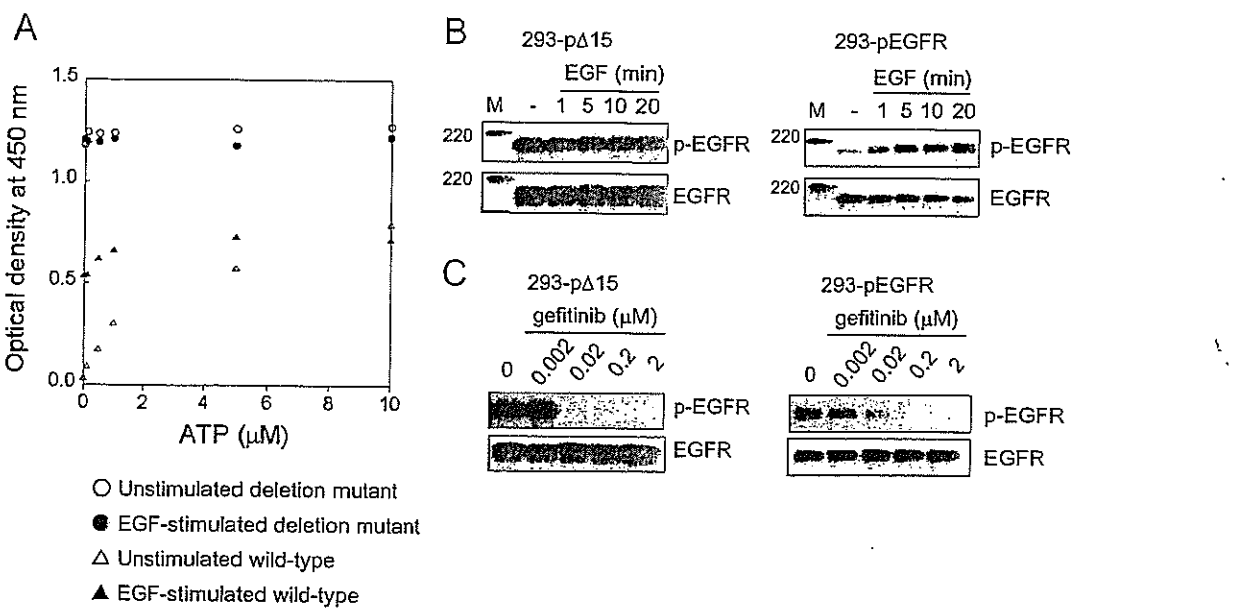

Figure 1 Autophosphorylation reactions of deletion mutant EGFR and wild-type EGFR

(A) The 293-pΔ15 and 293-pEGFR cells were treated with or without EGF (100 ng/ml) for 10 min after serum-starvation. EGFR was extracted from the cells and immobilized on wells with anti-EGFR antibody. Autophosphorylation reactions were initiated by the addition of ATP, and autophosphorylation was detected using horseradish-peroxidase-conjugated phosphotyrosine antibody, measuring the absorbance ('optical density') at 450 nm. Autophosphorylation was seen for unstimulated (○) and EGF-stimulated (●) deletion mutant EGFR, and unstimulated (△) and EGF-stimulated (▲) wild-type EGFR. Results are representative of at least three independent experiments. (B) The 293-pΔ15 and 293-pEGFR cells were treated with or without EGF (100 ng/ml) for the indicated times after serum-starvation. Phosphorylation of EGFR and total EGFR was determined by immunoblotting. (C) The 293-pΔ15 and 293-pEGFR cells were exposed to gefitinib (0.002–2 μM) for 3 h under serum-starvation conditions, and stimulated with EGF (100 ng/ml) for 10 min. The cells were then lysed and subjected to immunoblot analysis.

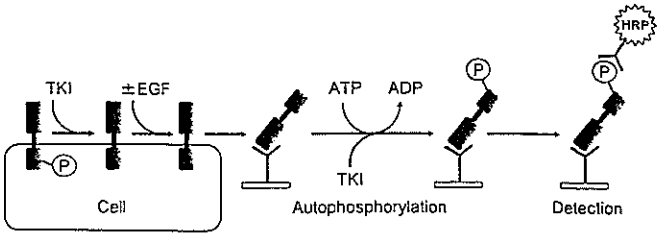

Figure 2 Schematic illustration of the cell-based autophosphorylation assay

The 293-pΔ15 and the 293-pEGFR cells overexpressing deletion mutant EGFR and wild-type EGFR respectively were treated with 2 μM gefitinib for 3 h and stimulated with or without EGF (100 ng/ml) under serum-starvation conditions. EGFR was extracted from cells and immobilized on wells with anti-EGFR antibody. The autophosphorylation reaction was initiated by the addition of ATP with or without gefitinib, and horseradish-peroxidase-conjugated anti-phosphotyrosine antibody was used to detect the phosphorylation of EGFR. TKI, tyrosine kinase inhibitor.

horseradish-peroxidase-conjugated anti-phosphotyrosine antibody, PY-99-HRP (0.4 μg/ml in PBS containing 1% BSA and 0.1% Tween 20) (Santa Cruz Biotechnology) was added to the wells for 2 h at room temperature. The wells were washed three times with TBS-T. Bound phosphotyrosine antibody was detected colorimetrically after adding 100 μl of substrate (tetramethylbenzidine and H_2O_2) to each well. After a 10 min incubation, the colour reaction was quenched by the addition of 100 μl of 1M H_2SO_4. The absorbance readings for each well were determined at 450 nm with Delta-soft on an Apple Macintosh computer interfaced to a Bio-Tek Microplate Reader EL-340 (BioMetallics).

Data analysis

For kinetic analysis, an Eadie–Hofstee plot was applied for the calculation of K_m (Michaelis constant) and V_{max} (maximum velocity). The data obtained were plotted as velocity against velocity/substrate concentration (V/ATP). The slope of the line is equal to $-K_m$ and the x-intercept is V_{max}. The K_i value was calculated as follows:

$$K_i = (K_m \times [I])/(K_{m,I} - K_m) \quad (1)$$

in which K_m is the Michaelis constant for ATP, $K_{m,I}$ is the Michaelis constant for ATP in the presence of gefitinib and [I] is the concentration of gefitinib. The statistical analysis was performed using KaleidaGraph (Synergy Software).

RESULTS

Autophosphorylation of deletion mutant EGFR and wild-type EGFR

We performed the autophosphorylation assay and immunoblot analysis using lysates extracted from 293-pΔ15 and 293-pEGFR cells under unstimulated and EGF-stimulated conditions (Figures 1A and 1B). Under unstimulated conditions, deletion mutant EGFR was highly phosphorylated in the absence of ATP. Addition of ATP did not affect the autophosphorylation of deletion mutant EGFR. On the other hand, autophosphorylation of wild-type EGFR was barely detectable without ATP, and proceeded in an ATP-dependent manner. In the EGF-stimulated case, wild-type EGFR was phosphorylated to a greater extent in the absence of ATP than unstimulated wild-type EGFR. The autophosphorylation of EGF-stimulated wild-type EGFR additively increased with the addition of ATP. These findings indicate that the deletion mutant retains the constitutive activity in our autophosphorylation assay. In the immunoblot analysis, phosphorylation of deletion mutant EGFR was detected in 293-pΔ15 cells without ligand stimulation. Addition of EGF increased phosphorylation of EGFR in the 293-pEGFR cells. Taken together, these results indicate that the deletion mutant has constitutive autophosphorylation activity.

In addition, we examined the secretion of major ligands for EGFR such as EGF and TGF-α from transfected HEK-293 cells by ELISA. No detectable EGF and TGF-α secretion was observed in the cultivation medium used for HEK-293 transfectants (results not shown), indicating that these transfectants are not activated via EGF-mediated autocrine loops. We considered that autophosphorylation using unstimulated EGFR represents a

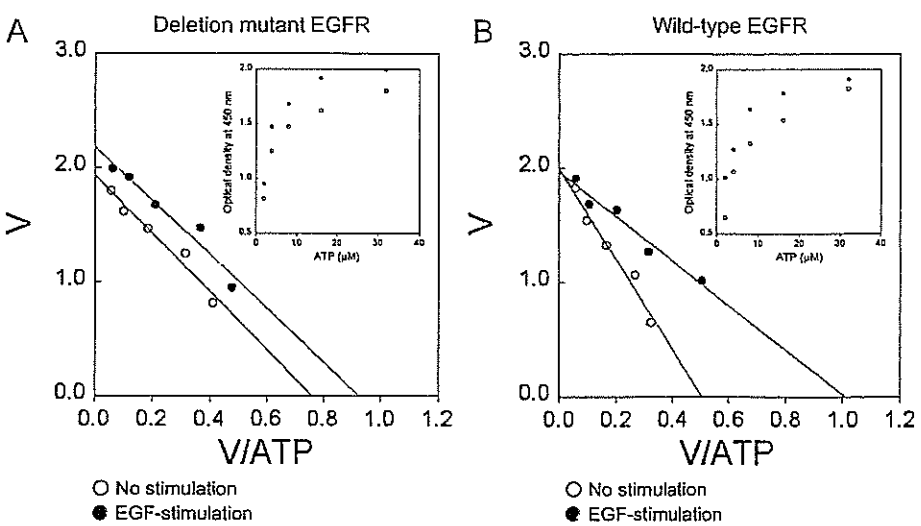

Figure 3 Autophosphorylation activities of deletion mutant EGFR and wild-type EGFR

Plots of absorbance ('optical density') against ATP concentration (inset) were fitted to an Eadie–Hofstee plot to calculate the values of kinetic parameters (K_m and V_{max}) for deletion mutant EGFR (**A**) and wild-type EGFR (**B**) under unstimulated (○) and EGF-stimulated conditions (●). Results are representative of at least three independent experiments with similar results.

Table 1 Kinetic parameters for ATP

The autophosphorylation reaction was performed using the indicated enzyme and gefitinib (0.5–5 nM). The steady-state kinetic parameters for ATP were determined from the Eadie–Hofstee plot in Figure 5. Results are means ± S.D. for three independent duplicate experiments.

		K_m (μM)				V_{max} (μM · min^{-1})			
		Deletion mutant		Wild-type		Deletion mutant		Wild-type	
Gefitinib (nM)	EGF stimulation ...	−	+	−	+	−	+	−	+
0		2.5 ± 0.2	2.2 ± 0.2	4.0 ± 0.3	1.9 ± 0.1	1.9 ± 0.1	2.1 ± 0.1	2.0 ± 0.0	1.9 ± 0.0
0.5		5.6 ± 0.5	5.7 ± 0.4	4.1 ± 0.4	2.3 ± 0.1	1.9 ± 0.1	1.9 ± 0.2	2.0 ± 0.1	1.9 ± 0.1
1		9.8 ± 2.8	10.9 ± 3.0	4.6 ± 1.2	2.5 ± 0.1	2.0 ± 0.1	1.9 ± 0.0	2.0 ± 0.2	1.8 ± 0.1
5		26.1 ± 5.4	30.2 ± 4.2	7.0 ± 2.3	4.9 ± 0.9	1.9 ± 0.1	1.8 ± 0.2	2.0 ± 0.1	1.8 ± 0.2

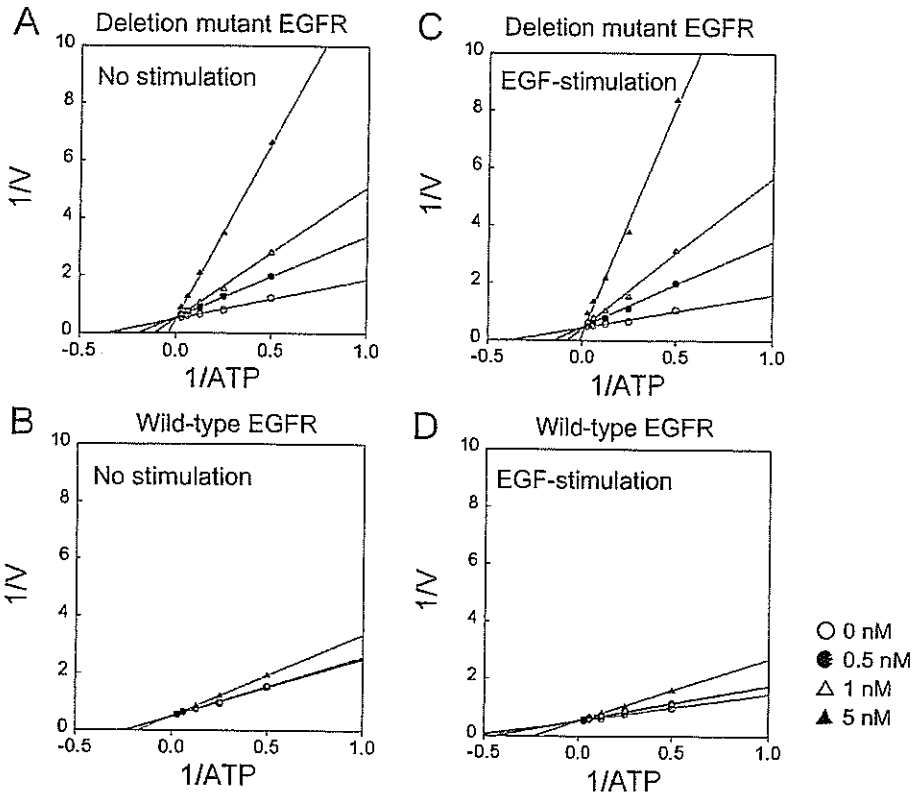

Figure 4 Mechanism of inhibition of deletion mutant EGFR by gefitinib

Autophosphorylation of unstimulated deletion mutant (**A**), unstimulated wild-type (**B**), EGF-stimulated deletion mutant (**C**) and EGF-stimulated wild-type (**D**) EGFR was measured with or without gefitinib at concentrations of 0 (○), 0.5 (●), 1 (△) and 5 (▲) nM. Reciprocal velocity against reciprocal ATP concentrations (0.5–32 μM) were plotted. Data are representative of at least three independent experiments.

low level of EGF-independent basal phosphorylation, whereas autophosphorylation using EGF-stimulated EGFR represents EGF-induced phosphorylation.

Kinetic parameters of autophosphorylation

The deletion mutant EGFR is constitutively phosphorylated under unstimulated conditions. Measuring the autophosphorylation activity of deletion mutant EGFR requires unphosphorylated tyrosine residues of EGFR. An autophosphorylation assay was reconstructed to determine the kinetic parameters of deletion mutant EGFR. The method is summarized in Figure 2. The concentrations of gefitinib used (2 μM) completely inhibited phosphorylation of both the deletion mutant and wild-type EGFR, as demonstrated by immunoblot analysis (Figure 1C). We performed autophosphorylation assays with various amounts of EGFR (results not shown). In our autophosphorylation assay, a constant amount of EGFR (130 ng/well) was adopted to measure its autophosphorylation, because this amount of EGFR was found to be appropriate for detecting changes in the absorbance of both wild-type and deletion mutant EGFR. The autophosphorylation of deletion mutant EGFR and wild-type EGFR was analysed by comparison with unstimulated and EGF-stimulated EGFR (Figure 3). The higher phosphorylation of deletion mutant EGFR shown in Figure 1(A) was lowered by using gefitinib-treated lysates, while the autophosphorylation reaction was initiated by addition of ATP. The ATP-dependent autophosphorylation reactions of deletion mutant EGFR and wild-type EGFR in crude cellular extracts were monitored (Figure 3, insets). The data were transformed into an Eadie–Hofstee plot, and the kinetic parameters were determined as apparent K_m and V_{max} values for ATP (Figure 3 and Table 1). Under unstimulated conditions,

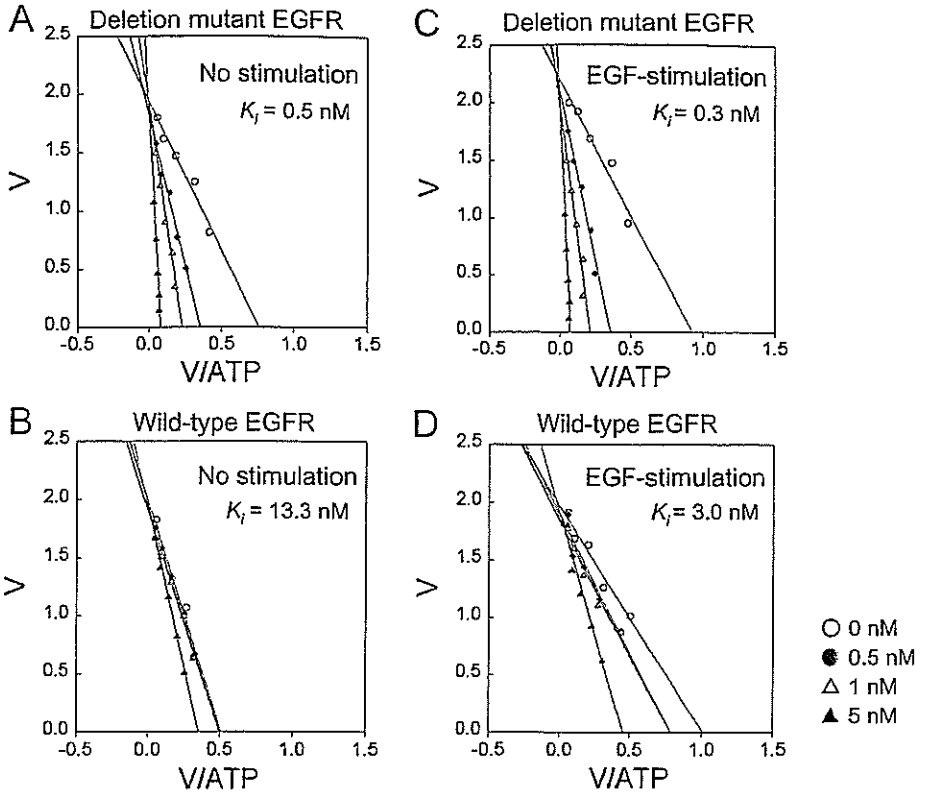

Figure 5 Inhibition constant of gefitinib for autophosphorylation activity of deletion mutant EGFR

The same dataset as shown in Figure 4 was fitted to an Eadie–Hofstee plot, and kinetic parameters from this fit are summarized in Table 1. Shown are the results for the unstimulated (**A**) and EGF-stimulated (**C**) deletion mutant EGFR and unstimulated (**B**) and EGF-stimulated (**D**) wild-type EGFR in response to ATP with or without gefitinib at concentrations of 0 (○), 0.5 (●), 1 (△) and 5 (▲) nM. Results are representative of at least three independent experiments.

differences in activities were seen between unstimulated wild-type (K_m for ATP = 4.0 ± 0.3 μM) and deletion mutant EGFR (K_m for ATP = 2.5 ± 0.2 μM). Under EGF-stimulated conditions, there was no difference in K_m values between EGF-stimulated wild-type EGFR (K_m for ATP = 1.9 ± 0.1 μM) and deletion mutant EGFR (K_m for ATP = 2.2 ± 0.2 μM). The V_{max} values of wild-type EGFR and deletion mutant EGFR were equal under both conditions. These results suggest that the wild-type EGFR is conformationally activated by EGF stimulation, and that the mutant EGFR is active without ligand stimulation.

Gefitinib inhibits autophosphorylation of deletion mutant EGFR

We examined the inhibitory effect of gefitinib (0.5, 1 and 5 nM) on the autophosphorylation of deletion mutant EGFR in comparison with wild-type EGFR under unstimulated and EGF-stimulated conditions. The data were transformed into a Lineweaver–Burk plot for estimation of the mode of inhibition (Figure 4). Lineweaver–Burk plot analysis showed that gefitinib competitively inhibited the autophosphorylation of deletion mutant EGFR as well as that of wild-type EGFR. The data were transformed into an Eadie–Hofstee plot for determination of kinetic parameters (Figure 5). Eadie–Hofstee plot analysis revealed the apparent K_m and V_{max} values for ATP in the presence of various gefitinib concentrations, and the kinetic parameters are summarized in Table 1. The K_i for deletion mutant EGFR and wild-type EGFR was calculated using eqn 1 (see the Materials and methods section). The K_i value of gefitinib for deletion mutant EGFR (K_i for gefitinib = 0.5 ± 0.1 nM) was 26-fold lower than that for wild-type EGFR (K_i for gefitinib = 13.3 ± 5.1 nM) under unstimulated conditions (Figure 5). Under EGF-stimulated conditions, the K_i value of gefitinib for deletion mutant EGFR (0.3 ± 0.1 nM) was 10-fold lower than that for wild-type EGFR (3.0 ± 0.6 nM) (Figure 5). Based on these comparative studies, we concluded that gefitinib binds deletion mutant EGFR more strongly than wild-type EGFR. In addition, we calculated the inhibitory effect of gefitinib for both types of EGFR in the presence of 2 μM ATP (Figure 6). Relatively strong inhibitory activity was detected for deletion mutant EGFR as compared with wild-type EGFR. These results suggest that gefitinib had a high affinity (low K_i value) for deletion mutant EGFR compared with wild-type EGFR.

DISCUSSION

Wild-type EGFR is unphosphorylated, being in an inactive form, under unstimulated conditions. The binding of ligands to the extracellular domain of EGFR induces dimerization and phosphorylation of the receptor into the active form [13]. The kinetic parameters of wild-type EGFR in our autophosphorylation assay are consistent with those of previous reports [14,15]. Crystallographic analysis has shown that the structure of the EGFR kinase domain after forming a complex with erlotinib exhibits a conformation consistent with the active form of protein kinases [16,17]. Previously, we reported that the deletion mutant EGFR was dimerized and phosphorylated constitutively without ligand stimulation, suggesting an active conformation [9]. We analysed the enzymatic properties of the deletion mutant EGFR, and

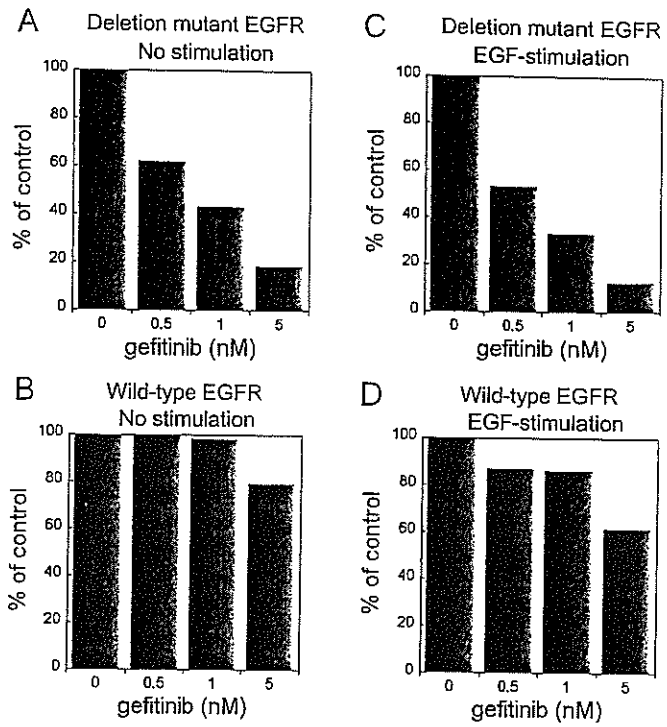

Figure 6 Effects of gefitinib on autophosphorylation of deletion mutant EGFR

The percentage of absorbance compared with the control under conditions of 2 μM ATP was calculated using the same dataset as shown in Figure 4 at a concentration of 2 μM ATP. The results shown are for unstimulated (**A**) and EGF-stimulated (**C**) deletion mutant EGFR and unstimulated (**B**) and EGF-stimulated (**D**) wild-type EGFR in response to ATP with or without gefitinib. Results are representative of at least three independent experiments.

determined the K_i value of gefitinib for deletion mutant EGFR. The inhibition constant of gefitinib for wild-type EGFR was similar to the value reported by Wakeling et al. [18]. We showed that the K_i value of gefitinib for deletion mutant EGFR was much lower than that for wild-type EGFR. The evidence of the decreased K_i value of gefitinib for deletion mutant EGFR means that gefitinib binds deletion mutant EGFR more strongly than wild-type EGFR. The high-affinity interaction between deletion mutant EGFR and gefitinib may be attributable to structural differences between deletion mutant EGFR and wild-type EGFR.

Our conclusion does not contradict the previous report by Stamos et al. [16] on a similar EGFR-targeted tyrosine kinase inhibitor, erlotinib, which binds to the active form of EGFR [14]. This result differs from that reported elsewhere: Fabian et al. [19] reported that there were no differences in the binding affinity of EGFR-targeted tyrosine kinase inhibitors between wild-type EGFR and mutant EGFR, including the deletion mutation. They constructed and expressed the kinase domain of EGFR on a bacteriophage surface, followed by interaction with immobilized inhibitors using biotin–avidin systems. Conversely, in our experiments, we performed autophosphorylation assays with EGFR extracted from 293-pΔ15 and the 293-pEGFR cells overexpressing deletion mutant and wild-type EGFR respectively. We consider our cell-based autophosphorylation assay results to reflect the native state of deletion mutant EGFR and to possibly explain the hypersensitivity of mutant-expressing cells to gefitinib.

We demonstrated that the deletion mutant actually binds gefitinib more strongly than wild-type EGFR. This is likely to be the mechanism of action of other tyrosine kinase inhibitors such as erlotinib, ZD6474 [dual inhibitor targeted to VEGFR2 (vascular endothelial growth factor receptor 2)/KDR (kinase insert domain-containing receptor) and EGFR] and other possible multi-targeted tyrosine kinase inhibitors. Indeed, EGFR-specific tyrosine kinase inhibitors AG1478 and erlotinib, as well as ZD6474, as described in our previous report [7] showed different growth-inhibitory activities against HEK-293 transfected with deletion mutant EGFR (results not shown). Thus it is likely that these (ATP competitive) tyrosine kinase inhibitors have different binding property effects on wild-type and deletion mutant EGFR to those of gefitinib.

In the present study, we focused on the enzymatic properties of in-frame deletion mutant EGFR (delE746–A750). The inhibition of receptor autophosphorylation in deletion mutant EGFR by gefitinib was much greater than that in wild-type EGFR. Next, it is necessary to examine the kinetic properties of other types of EGFR mutants, especially L858R, and these findings may pave the way for the discovery of different kinase inhibitors with different inhibition profiles for EGFR.

This work was supported by funds for the Third Term Comprehensive 10-Year Strategy for Cancer Control.

REFERENCES

1 Arteaga, C. L. (2003) ErbB-targeted therapeutic approaches in human cancer. Exp. Cell Res. **284**, 122–130
2 Traxler, P., Furet, P., Mett, H., Buchdunger, E., Meyer, T. and Lydon, N. (1997) Design and synthesis of novel tyrosine kinase inhibitors using a pharmacophore model of the ATP-binding site of the EGF-R. J. Pharm. Belg. **52**, 88–96
3 Shepherd, F. A., Rodrigues Pereira, J., Ciuleanu, T., Tan, E. H., Hirsh, V., Thongprasert, S., Campos, D., Maoleekoonpiroj, S., Smylie, M., Martins, R. et al. (2005) Erlotinib in previously treated non-small-cell lung cancer. N. Engl. J. Med. **353**, 123–132
4 Bell, D. W., Lynch, T. J., Haserlat, S. M., Harris, P. L., Okimoto, R. A., Brannigan, B. W., Sgroi, D. C., Muir, B., Riemenschneider, M. J., Iacona, R. B. et al. (2005) Epidermal growth factor receptor mutations and gene amplification in non-small-cell lung cancer: molecular analysis of the IDEAL/INTACT gefitinib trials. J. Clin. Oncol. **23**, 8081–8092
5 Lynch, T. J., Bell, D. W., Sordella, R., Gurubhagavatula, S., Okimoto, R. A., Brannigan, B. W., Harris, P. L., Haserlat, S. M., Supko, J. G., Haluska, F. G. et al. (2004) Activating mutations in the epidermal growth factor receptor underlying responsiveness of non-small-cell lung cancer to gefitinib. N. Engl. J. Med. **350**, 2129–2139
6 Paez, J. G., Janne, P. A., Lee, J. C., Tracy, S., Greulich, H., Gabriel, S., Herman, P., Kaye, F. J., Lindeman, N., Boggon, T. J. et al. (2004) EGFR mutations in lung cancer: correlation with clinical response to gefitinib therapy. Science **304**, 1497–1500
7 Arao, T., Fukumoto, H., Takeda, M., Tamura, T., Saijo, N. and Nishio, K. (2004) Small in-frame deletion in the epidermal growth factor receptor as a target for ZD6474. Cancer Res. **64**, 9101–9104
8 Tracy, S., Mukohara, T., Hansen, M., Meyerson, M., Johnson, B. E. and Janne, P. A. (2004) Gefitinib induces apoptosis in the EGFRL858R non-small-cell lung cancer cell line H3255. Cancer Res. **64**, 7241–7244
9 Sakai, K., Arao, T., Shimoyama, T., Murofushi, K., Sekijima, M., Kaji, N., Tamura, T., Saijo, N. and Nishio, K. (2005) Dimerization and the signal transduction pathway of a small in-frame deletion in the epidermal growth factor receptor. FASEB J. **20**, 311–313
10 Nishio, K., Arioka, H., Ishida, T., Fukumoto, H., Kurokawa, H., Sata, M., Ohata, M. and Saijo, N. (1995) Enhanced interaction between tubulin and microtubule-associated protein 2 via inhibition of MAP kinase and CDC2 kinase by paclitaxel. Int. J. Cancer **63**, 688–693
11 Kawamura-Akiyama, Y., Kusaba, H., Kanzawa, F., Tamura, T., Saijo, N. and Nishio, K. (2002) Non-cross resistance of ZD0473 in acquired cisplatin-resistant lung cancer cell lines. Lung Cancer **38**, 43–50
12 Koizumi, F., Shimoyama, T., Taguchi, F., Saijo, N. and Nishio, K. (2005) Establishment of a human non-small cell lung cancer cell line resistant to gefitinib. Int. J. Cancer **116**, 36–44
13 Tanner, K. G. and Kyte, J. (1999) Dimerization of the extracellular domain of the receptor for epidermal growth factor containing the membrane-spanning segment in response to treatment with epidermal growth factor. J. Biol. Chem. **274**, 35985–35990
14 Nair, N., Davis, R. J. and Robinson, H. L. (1992) Protein tyrosine kinase activities of the epidermal growth factor receptor and ErbB proteins: correlation of oncogenic activation with altered kinetics. Mol. Cell. Biol. **12**, 2010–2016

15 Wood, E. R., Truesdale, A. T., McDonald, O. B., Yuan, D., Hassell, A., Dickerson, S. H., Ellis, B., Pennisi, C., Horne, E., Lackey, K. et al. (2004) A unique structure for epidermal growth factor receptor bound to GW572016 (Lapatinib): relationships among protein conformation, inhibitor off-rate, and receptor activity in tumor cells. Cancer Res. **64**, 6652–6659
16 Stamos, J., Sliwkowski, M. X. and Eigenbrot, C. (2002) Structure of the epidermal growth factor receptor kinase domain alone and in complex with a 4-anilinoquinazoline inhibitor. J. Biol. Chem. **277**, 46265–46272
17 Noble, M. E., Endicott, J. A. and Johnson, L. N. (2004) Protein kinase inhibitors: insights into drug design from structure. Science **303**, 1800–1805
18 Wakeling, A. E., Guy, S. P., Woodburn, J. R., Ashton, S. E., Curry, B. J., Barker, A. J. and Gibson, K. H. (2002) ZD1839 (Iressa): an orally active inhibitor of epidermal growth factor signaling with potential for cancer therapy. Cancer Res. **62**, 5749–5754
19 Fabian, M. A., Biggs, 3rd, W. H., Treiber, D. K., Atteridge, C. E., Azimioara, M. D., Benedetti, M. G., Carter, T. A., Ciceri, P., Edeen, P. T., Floyd, M. et al. (2005) A small molecule-kinase interaction map for clinical kinase inhibitors. Nat. Biotechnol. **23**, 329–336

Received 12 December 2005/3 April 2006; accepted 20 April 2006
Published as BJ Immediate Publication 20 April 2006, doi:10.1042/BJ20051962

The FASEB Journal • FJ Express

Dimerization and the signal transduction pathway of a small in-frame deletion in the epidermal growth factor receptor

Kazuko Sakai,*,§ Tokuzo Arao,* Tatsu Shimoyama,* Kimiko Murofushi,§ Masaru Sekijima,|| Naoko Kaji,|| Tomohide Tamura,† Nagahiro Saijo,† and Kazuto Nishio*,‡,1

*Shien-Lab, Medical Oncology, †National Cancer Center Hospital and ‡Pharmacology Division, National Cancer Center Research Institute, Tokyo, Japan; and §Department of Biology, Faculty of Science, Ochanomizu University, Tokyo, Japan; and ||Mitsubishi Chemical Safety Institute Ltd., Ibaraki, Japan

To read the full text of this article, go to http://www.fasebj.org/cgi/doi/10.1096/fj.05-4034fje; doi: 10.1096/fj.05-4034fje

SPECIFIC AIM

A short, in-frame deletional mutant (E746-A750del) a major mutant form of EGFR in non-small cell lung cancer, and has been reported to be a major determinant of response to EGFR tyrosine kinase inhibitors such as gefitinib and erlotinib. However, the biological and pharmacological functions of mutational EGFR remain unclear. The aim of this study is to clarify whether it is constitutively active or not and whether alteration occurs downstream of the intracellular signaling.

PRINCIPAL FINDINGS

1. A short, in-frame deletional mutant (E746-A750del) induced dimerization and phosphorylation of EGFR without any ligand stimulation

To determine the biological functions of deletion mutant (E746-A750del) EGFR, we used the stable transfected cells of wild-type and deletion mutant of EGFR. Previously, we demonstrated that the 293(D) cells transfected with the deletional EGFR were hypersensitive to EGFR-targeted tyrosine kinase inhibitors such as gefitinib and ZD6474 as compared with the 293(W) cells transfected with wild-type EGFR. Dimerization and phosphorylation of EGFR in these cells were determined by using chemical cross-linker and by immunoblot analysis (**Fig. 1**). No expression of EGFR dimer or monomer was detected in the 293(M) cells. Increased dimerization and phosphorylation of the deletional EGFR with a molecular weight of ~400 kDa were detected without EGF stimulation in the 293(D) cells. When stimulated with the EGF, increased dimerized and phosphorylated EGFR were observed in the 293(W) cells, whereas no response of EGFR to EGF was observed in the 293(D) cells. The ratio of dimerized to monomeric EGFR in 293(W) and 293(D) cells was analyzed densitometrically (Fig. 1, right). The dimer/monomer ratio in the 293(W) cells was markedly increased (~3-fold) by addition of EGF. Under unstimulated conditions, the dimer/monomer ratio of the 293(D) cells was higher than that of the 293(W) cells and the ratio was unchanged by addition of EGF. These results suggest that the cells expressing the wild-type of EGFR responded to EGF for their dimerization and phosphorylation and that the deletional mutant of EGFR was dimerized and phosphorylated constitutively without any ligand stimulation.

2. p44/42 MAPK and AKT pathways are activated in the cells expressing deletional EGFR without ligand stimulation

We examined the phosphorylation status of p44/42 MAPK and AKT that are major downstream targets of EGFR in the transfectants. Even under unstimulated conditions, increased phosphorylation of p44/42 MAPK and AKT was observed in the 293(D) cells. In the 293(W) cells, increased phosphorylation of p44/42 MAPK and AKT was observed with the addition of EGF but p44/42 MAPK was remarkably phosphorylated. On the other hand, no increased phosphorylation of p44/42 MAPK and AKT was observed with the addition of EGF in the 293(D) cells. This result suggests that the p44/42 MAPK and AKT pathways are activated in cells expressing the deletional EGFR without ligand stimulation.

[1] Correspondence: Shien-Lab, Medical Oncology, National Cancer Center Hospital, Tsukiji 5-1-1, Chuo-ku, Tokyo 104-0045, Japan. E-mail: knishio@gan2.res.ncc.go.jp

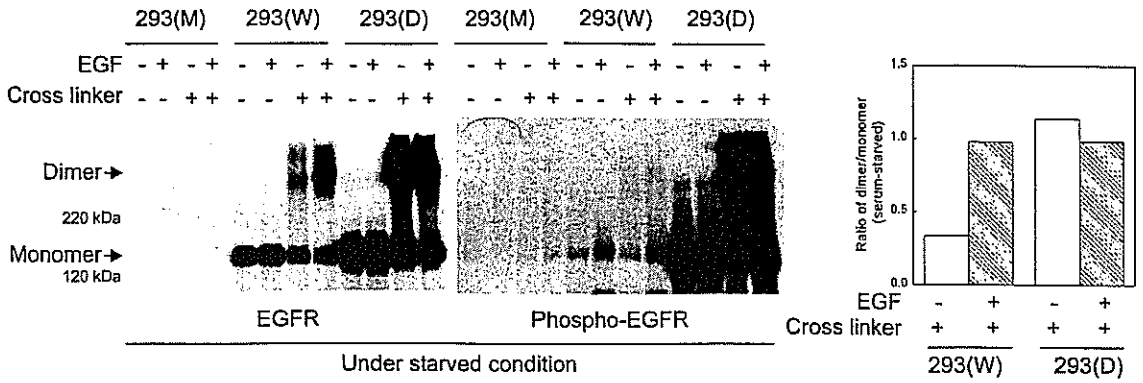

Figure 1. Dimerization and phosphorylation of wild-type EGFR and deletional EGFR A. The 293 cells transfected with the empty vector (293(M)), wild-type EGFR (293(W)), and deletional EGFR (293(D)) were treated with or without EGF (10 ng/mL) for 10 min after serum starvation. After two washes with ice-cold PBS(+), monolayer cells were incubated with the chemical cross-linking reagent BS^3 (1.5 mM) in PBS(+). Glycine (20 mM) was added for an additional 5 min to terminate the reaction. The lysates (twenty μg protein) were subjected to 2–15% SDS-PAGE followed by immunoblot analysis using anti-EGFR and anti-phospho-EGFR. Right panel: ratio of dimerized to monomeric EGFR.

3. Gefitinib inhibited the AKT signaling pathway more strongly than the p44/42 MAPK signaling pathway

We next determined the action of EGFR-targeted tyrosine kinase inhibitor gefitinib on downstream of deletional EGFR (**Fig. 2A**). In the 293(W) cells, phosphorylation of p44/42 MAPK was not inhibited by exposure to a low dose of gefitinib (0.01 μM) but phosphorylation of AKT was inhibited by exposure to gefitinib (~70%, Fig. 2*C*). In contrast, exposure to gefitinib decreased phospho-EGFR in the 293(D) cells. Phosphorylation of AKT was completely inhibited by 0.01 μM gefitinib exposure (~99%, Fig. 2*C*), whereas inhibition of p44/42 MAPK phosphorylation was not remarkable in the 293(D) cells (~20%, Fig. 2*B*). These data suggest that gefitinib inhibited the AKT signaling pathway more strongly than the p44/42 MAPK signaling pathway in the cells expressing the deletion mutant EGFR.

4. AKT pathway was activated in the PC-9 cells expressing deletional EGFR intrinsically

To examine whether increased phosphorylation is also observed in the lung cancer cells intrinsically expressing deletional EGFR, we monitored the phosphorylation of EGFR and its related molecules in the PC-9 cells expressing deletional EGFR by using a beads-based mulitiplex assay. We found increased phosphorylation of EGFR and downstream molecules of AKT pathway including IκB-α in PC-9 cells. This finding is consistent with the result of the previous experiments with the 293(D) cells. It is suggested that AKT pathway is activated in the cells expressing deletional EGFR intrinsically.

CONCLUSIONS AND SIGNIFICANCE

To clarify the function of deletional EGFR, we used the cell transfectants with deletional EGFR [293(D)] that is

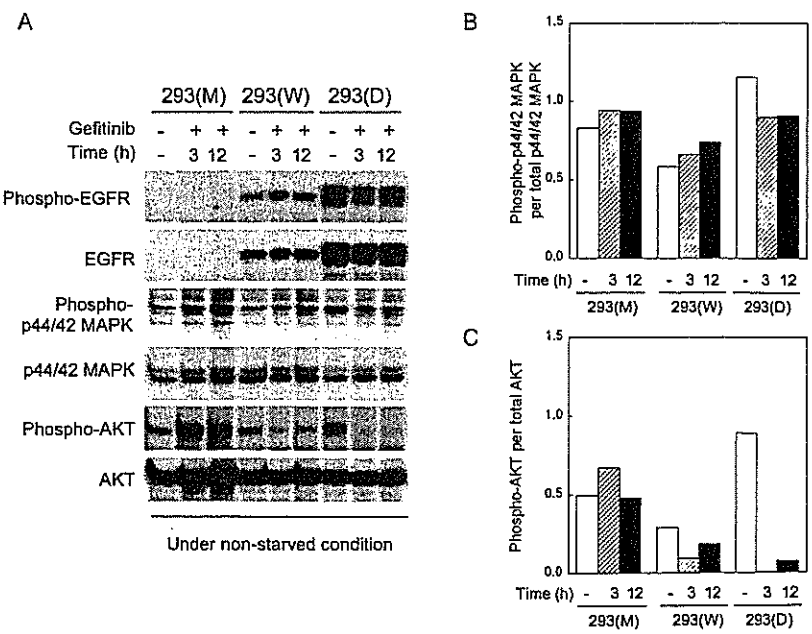

Figure 2. Effect of gefitinib on phosphorylation of EGFR, p44/42 MAPK, and AKT in the EGFR transfected 293 cells. *A)* The 293(M), 293(W), and 293(D) cells were incubated with gefitinib (0.01 μM) for 3 h or 12 h under nonstarved conditions. After two washes with ice-cold PBS(+), monolayer cells were lysed. Equivalent amounts of protein were separated by 2–15% gradient SDS-PAGE for EGFR or 10–20% for p44/42 MAPK, phospho-p44/42 MAPK, AKT, and phospho-AKT, then subjected to immunoblot analysis. *B)* Histogram of the degree of p44/42 MAPK activation expressed as phospho-p44/42 MAPK per total p44/42 MAPK. *C)* Histogram of the degree of AKT activation expressed as phospho-AKT per total AKT.

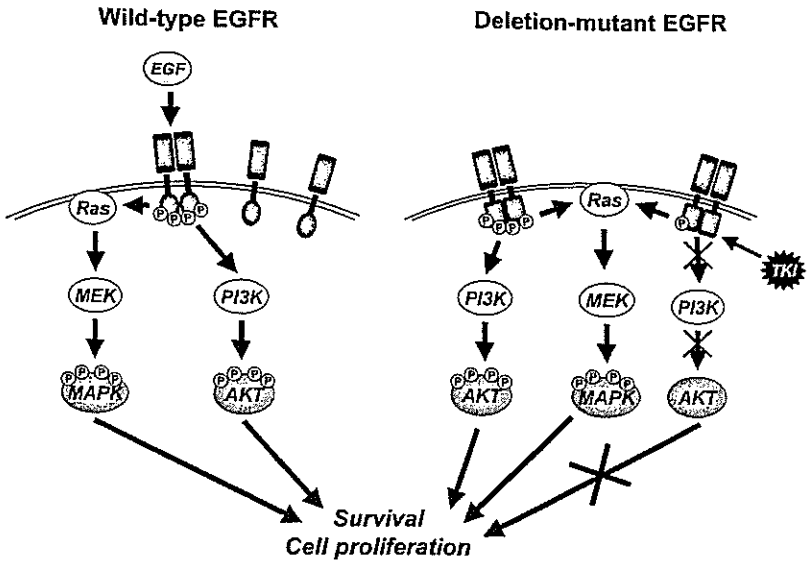

Figure 3. Function of deletional EGFR. Wild-type EGFR is dimerized and phosphorylated by EGF the wild-type EGFR and MAPK and AKT pathways are activated. The deletion mutant EGFR is dimerized and phosphorylated without EGF. Both MAPK and AKT pathways are activated; but phospho-AKT was inhibited by TKI predominantly in the cells expressing deletional EGFR. MEK, MAP kinase/extracellular regulated kinases; PI3K, phosphoinositide-3-kinase; TKI, tyrosine kinase inhibitors.

hypersensitive to tyrosine kinase inhibitors (e.g., gefitinib). We detected significantly higher levels of dimerization and phosphorylation of deletional EGFR without any ligand stimulation in the cells deletional EGFR. Increased phosphorylation of p44/42 MAPK and AKT was observed in the 293(D) cells. These results suggest that deletional EGFR is constitutively active. When the 293(D) cells were exposed to gefitinib (0.01 μM), AKT phosphorylation was completely suppressed, suggesting that deletional EGFR signaling inclines toward the AKT pathways. A summary of characteristics of deletional EGFR is shown in Fig. 3.

An additional experiment using a PC-9 lung cancer cell line intrinsically expressing deletional EGFR confirmed the gain of function of deletional EGFR and activated AKT signaling pathway.

Results from this study have provided the understanding for biological functions of deletional EGFR and cellular hypersensitivity to the EGFR-targeted tyrosine kinase inhibitor.

Now over 30 types of mutation have been reported in clinical lung cancer specimens. We will examine the biological function of other types of EGFR mutants differentially, with the aim of selecting clinically meaningful mutations. FJ

EGFR Mutation of Tumor and Serum in Gefitinib-Treated Patients with Chemotherapy-Naive Non–small Cell Lung Cancer

Hideharu Kimura, MD, Kazuo Kasahara, MD, Kazuhiko Shibata, MD, Takashi Sone, MD, Akihiro Yoshimoto, MD, Toshiyuki Kita, MD, Yukari Ichikawa, MD, Yuko Waseda, MD, Kazuyoshi Watanabe, MD, Hiroki Shiarasaki, MD, Yoshihisa Ishiura, MD, Masayuki Mizuguchi, MD, Yasuto Nakatsumi, MD, Tatsuhiko Kashii, MD, Masashi Kobayashi, MD, Hideo Kunitoh, MD, Tomohide Tamura, MD, Kazuto Nishio, MD, Masaki Fujimura, MD, and Shinji Nakao, MD

Background: The authors evaluate the efficacy and safety of gefitinib monotherapy in chemotherapy-naive patients with advanced non small-cell lung cancer (NSCLC). A secondary endpoint is to evaluate the relationship between clinical manifestations and epidermal growth factor receptor (*EGFR*) mutation status.

Methods: Japanese chemotherapy-naive NSCLC patients were enrolled. They had measurable lesions. Eastern Cooperative Oncology Group performance status of 0 to 2, and adequate organ and bone marrow function. Patients received 250 mg of oral gefitinib daily. *EGFR* mutations in exon 18, 19, and 21 of DNA extracted from tumor and serum were analyzed by genomic polymerase chain reaction and direct sequence.

Results: All 30 patients were eligible for the assessment of efficacy and safety. An objective response and stable disease were observed in 10 patients (33.3%) and nine patients (30.0%), respectively. The median time to progression was 3.3 months and the median overall survival was 10.6 months. The 1-year survival rate was 43.3%. Grade 3 toxicities were observed in seven patients. *EGFR* mutation was observed in four of 13 (30.8%) tumors, and two of them achieved partial response. In serum samples, three of 10 patients with *EGFR* mutations in the serum before treatment had a response to gefitinib. *EGFR* mutation was observed in 10 of 27 and significantly more frequently observed in the posttreatment samples from patients with a partial response or stable disease than in those from patients with progressive disease ($p = 0.006$).

Conclusions: Gefitinib monotherapy in chemotherapy-naive NSCLC patients was active, with acceptable toxicities. These results warrant further evaluation of gefitinib monotherapy as a first-line therapy. The *EGFR* mutation in serum DNA may be a biomarker for monitoring the response to gefitinib during treatment.

Key Words: Non-small-cell lung cancer, Gefitinib, Epidermal growth factor receptor, Mutation, Serum DNA.

(*J Thorac Oncol.* 2006;1: 260–267)

Non-small-cell lung cancer (NSCLC) is the leading cause of cancer death in Japan and throughout the world.[1] Unfortunately, the majority of patients with NSCLC present with locally advanced or metastatic disease at the time of diagnosis. Although chemotherapy has produced modest survival benefits in advanced NSCLC patients, the outcome of chemotherapy for NSCLC remains unsatisfactory.

Protein tyrosine kinases play important roles in the pathogenesis of malignant tumors.[2] Among them, epidermal growth factor receptor (EGFR) tyrosine kinase has been implicated in the initiation and progression of NSCLC.[3–5] The overexpression of EGFR is frequent in NSCLC.[6] Monoclonal antibodies and low-molecular-weight compounds that inhibit the EGFR signaling pathway have been developed and shown to have antitumor effects. Gefitinib (Iressa, AstraZeneca, London, England) is an orally active EGFR type tyrosine kinase inhibitor. In four phase I studies, tumor shrinkage or stabilization after gefitinib monotherapy was observed in some patients with NSCLC. In two phase II trials, Iressa Dose Evaluation in Advanced Lung cancer (IDEAL) 1 and 2, gefitinib monotherapy was shown to have a substantial effect in NSCLC patients treated previously with chemotherapy.[7,8] In these trials, patients of Asian origin and who had never been smokers had a statistically significant improvement in overall survival. In spite of encouraging results in the IDEAL trials, two large-scale, phase III, randomized trials, Iressa NSCLC Trial Assessing Combination Treatment, failed to show any survival benefit for the use of gefitinib.[9,10] Patients in a large-scale phase III trial comparing gefitinib

From Respiratory Medicine, Kanazawa University Hospital, Ishikawa; Internal Medicine, Kouseiren Takaoka Hospital, Takaoka; Internal Medicine, Shinminato Municipal Hospital, Shinminato, Japan; Internal Medicine, Fukuiken Saiseikai Hospital; Respiratory Medicine, Toyama City Hospital, Toyama; Respiratory Medicine, Ishikawa Prefectoral Hospital, Kanazawa; Respiratory Medicine, Kanazawa Municipal Hospital; Kanazawa; and National Cancer Center Hospital, and National Cancer Center Research Institute, Tokyo, Japan.

Address for correspondence: Kazuo Kasahara, MD, Takara-machi 13-1, Kanazawa, Ishikawa, Japan; email: kasa1237@med3.m.kanazawa-u.ac.jp

ISSN: 1556-0864/06/0103-0260

and placebo in advanced NSCLC with prior chemotherapy demonstrated in preliminary analysis a tendency to have improvement in overall survival but did not have a statistically significant improvement in overall survival.[11] There are many issues that need to be addressed with regard to the clinical application of gefitinib; one of the most important issues is the efficacy of gefitinib monotherapy in patients with chemotherapy-naive NSCLC,[12] and another is to establish a way to predict response to gefitinib.

Recently, it has been suggested that mutations in the EGFR tyrosine kinase domain play a critical role in determining tumor response to gefitinib in NSCLC patients.[13,14] The mutations consisted of small, in-frame deletions or substitutions clustered around the adenosine triphosphate binding site in exons 18, 19, and 21 of the *EGFR*. After these reports, some investigators supported the belief that *EGFR* mutation is one of the strong determinants of tumor response to gefitinib.[15–17] Tumors with *EGFR* mutations tend to be more common in adenocarcinomas, female patients, nonsmokers, and those of Asian origin. In most of those studies, tumor samples that were resected by operations were used. Because it is often difficult to obtain a tumor sample from an inoperable NSCLC patient, it is necessary to establish a method for detecting mutant *EGFR* from a patient sample other than from tumor specimens.

Polymerase chain reaction (PCR) technology for the amplification of small amounts of DNA has made it possible to identify the same alterations typically observed in DNA from serum samples from NSCLC patients.[18,19] Serum DNA may provide a noninvasive and repeatable source of genotypic information that could influence treatment and prognosis, especially in advanced NSCLC patients who have received gefitinib therapy. We essentially consider that it is possible to detect the *EGFR* mutation in serum DNA. We hypothesized that serum DNA may provide useful information on *EGFR* mutations in lung cancer patients.

As described above, the usefulness of gefitinib monotherapy is controversial and that in patients without pretreatment is unclear. Because *EGFR* mutations have been shown to be strongly associated with the response of NSCLC patients to gefitinib treatment, the analysis of *EGFR* mutations is necessary to evaluate the clinical benefit of gefitinib. We therefore conducted a multicenter phase II trial for these patients. The primary objective was to evaluate the objective response rate, and secondary objectives were to estimate the disease control rate, disease-related symptom improvement rate, safety, time to progression (TTP), and overall survival (OS). In addition, as a correlative study, we planned to detect *EGFR* mutations in serum samples from NSCLC patients and evaluate the relationship between the *EGFR* mutation and clinical manifestations in NSCLC patients receiving gefitinib treatment.

PATIENTS AND METHODS

Patient Eligibility

Patients who had histologically or cytologically proven stage IIIb or IV NSCLC and no previous chemotherapy were enrolled into this trial. Radiotherapy for metastatic lesions until 3 weeks before entry was allowed on condition that these lesions were not assessed for tumor response. Patients in whom recurrence occurred after surgery were also eligible. Patient eligibility criteria included at least one measurable lesion, age of 20 years or older, Eastern Cooperative Oncology Group performance status (PS) of 0 to 2, and life expectancy of greater than or equal to12 weeks. Adequate organ and bone marrow function was necessary, defined as leukocyte counts greater than or equal to 3.0×10^6/liter, neutrophil counts greater than or equal to 1.5×10^6/liter, platelet counts greater than or equal to 100×10^9/liter, hemoglobin levels greater than or equal to 8.5 g/dl, alanine aminotransferase or aspartate aminotransferase levels less than or equal to two times the upper limit of the reference range (<100 IU/liter in the presence of liver metastases), serum bilirubin levels less than or equal to 1.5 mg/dl, serum creatinine levels less than or equal to1.5 mg/dl, and PaO_2 levels greater than or equal to 65 mmHg. Patients with any of the following were excluded: active double cancer; severe complications such as myocardial infarction within 3 months before entry or uncontrolled diabetes; symptomatic brain or bone metastasis; diarrhea more severe than grade 2 according to National Cancer Institute Common Toxicity Criteria version 2; systemic administration of steroids to treat skin diseases; pleural, pericardial, or peritoneal effusion requiring treatment; and pregnancy or lactation. All patients were required to give informed consent.

Treatment

Patients were treated with gefitinib 250 mg orally once per day. Treatment was discontinued when the disease progressed, intolerable toxicities appeared, the patients requested withdrawal, or disease-related symptoms worsened without tumor response after 8 weeks of gefitinib monotherapy. These patients received chemotherapeutic treatment after gefitinib therapy. The chemotherapy regimen consisted of platinum (cisplatin or carboplatin) plus new agents (paclitaxel, docetaxel, gemcitabine, vinorelbine, or irinotecan) in patients aged 74 years or younger and vinorelbine monotherapy in patients aged 75 years or older. If symptomatic bone or brain metastasis occurred during gefitinib monotherapy, patients received radiotherapy after gefitinib treatment.

Efficacy and Drug-Related Adverse Events

Tumor size was assessed with computed tomography or magnetic resonance imaging scans every 4 weeks from the start to cessation of protocol treatment, using Response Evaluation Criteria in Solid Tumors guidelines.[20] Disease control was judged when patients achieved the best response of complete response, partial response (PR), or stable disease (SD), which was confirmed and sustained for 4 weeks. TTP was measured as the period from the start of the treatment to an identifiable time of disease progression. OS was measured from the start of the treatment until death or the last follow-up. The Kaplan-Meier method was used to calculate these measures.

Drug adverse events were recorded and graded according to National Cancer Institute Common Toxicity Criteria